NASA TN D-952

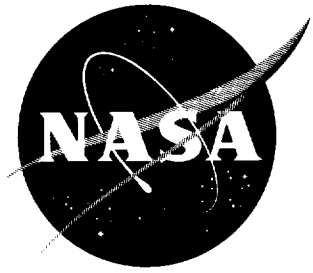

TECHNICAL NOTE

D-952

ANALYSIS OF EFFECTS OF INTERCEPTOR ROLL PERFORMANCE AND MANEUVERABILITY ON SUCCESS OF COLLISION-COURSE ATTACKS

By William H. Phillips

Langley Research Center
Langley Field, Va.

NATIONAL AERONAUTICS AND SPACE ADMINISTRATION

WASHINGTON August 1961

1D

NATIONAL AERONAUTICS AND SPACE ADMINISTRATION

TECHNICAL NOTE D-952

ANALYSIS OF EFFECTS OF INTERCEPTOR ROLL PERFORMANCE AND MANEUVERABILITY ON SUCCESS OF COLLISION-COURSE ATTACKS[1]

By William H. Phillips

SUMMARY

An attempt has been made to determine the importance of rolling performance and other factors in the design of an interceptor which uses collision-course tactics. A graphical method is presented for simple visualization of attack situations. By means of diagrams showing vectoring limits, that is, the ranges of interceptor position and heading from which attacks may be successfully completed, the relative importance of rolling performance and normal-acceleration capability in determining the success of attacks is illustrated. The results indicate that the reduction in success of attacks due to reduced rolling performance (within the limits generally acceptable from the pilots' standpoint) is very small, whereas the benefits due to substantially increasing the normal-acceleration capability are large.

Additional brief analyses show that the optimum speed for initiating a head-on attack is often that corresponding to the upper left-hand corner of the V-g diagram. In these cases, increasing speed beyond this point for given values of normal acceleration and radar range rapidly decreases the width of the region from which successful attacks can be initiated. On the other hand, if the radar range is increased with a variation somewhere between the first and second power of the interceptor speed, the linear dimensions of the region from which successful attacks can be initiated vary as the square of the interceptor speed.

INTRODUCTION

The present roll requirements for fighter airplanes are based largely on pilots' opinions of the rolling ability required for normal flying and maneuvering. In an attempt to relate the requirements more closely to tactical needs, flight and analytical studies were conducted

[1]Supersedes the recently declassified NACA Research Memorandum L58E27, by William H. Phillips, 1958.

previously to determine the roll requirements for pursuit-type tracking and for evasive action (ref. 1). Many present and proposed interceptors, however, do not use pursuit-type tactics, but, instead, use a collision-course attack which is better suited for firing rockets or missiles. An analysis of the roll requirements for these tactics was therefore considered desirable.

Detailed analyses (for example, those summarized in ref. 2) have been made in the past in order to obtain optimum interceptor systems utilizing collision-course attacks. These analyses have concentrated primarily on the design of the fire-control equipment rather than on the design of the interceptor. For this reason little information is available to evaluate the importance of roll performance on the effectiveness of an interceptor. In the present report, calculations are presented to show the relative effects of wide variations in the roll performance and normal-acceleration capability. Brief analyses are also included to show the effect on the success of attacks of other design factors such as speed and radar range.

SYMBOLS

a_l lateral component of acceleration measured in horizontal plane, g units

a_n normal acceleration, g units

b wing span

C_1, C_2 constants (see eq. (10))

C_{l_p} damping-in-roll coefficient, $\frac{\partial C_l}{\partial (pb/2V)}$

C_l rolling-moment coefficient, $\frac{\text{Rolling moment}}{qSb}$

C_N normal-force coefficient, $\frac{\text{Normal force}}{qS}$

g acceleration due to gravity

I_X moment of inertia of airplane about longitudinal axis

K_1, K_2 constants (see eq. (4))

K_c	constant (see eq. (2))
l_1	distance between detection of target and start of steady turn
l_2	distance between completion of turn and launching of missiles
l_3	distance traveled by missiles
M	Mach number
M_A	Mach number of attacker
p	rolling velocity, radians/sec
q	dynamic pressure, $\frac{\rho}{2} V^2$
R	radar range of attacker
r	radius of turn of attacker
S	wing area
t	time
T_1	time to start of constant-radius turn
T_o	time to reach a steady bank angle
T_{100}	time to roll through 100^o
V	true airspeed
V_A	attacker velocity
V_M	average missile velocity
V_T	target velocity
w	weight of attacker
y	lateral displacement between flight paths of target and attacker

γ	angle between flight paths of attacker and target at interception point (see fig. 1)
θ	angle between target flight path and line of sight (see fig. 1)
λ	angle between flight path of attacker and line of sight to target (look angle)
λ_{max}	maximum radar look angle of attacker
ρ	air density
τ	time constant in roll
ϕ	angle of bank
ϕ_o	final steady angle of bank
ψ	initial heading of attacker with respect to target path
ψ_c	heading of attacker for lead-collision course

Subscript:

max	maximum

Dot over quantity denotes differentiation with respect to time. Asterisk denotes distance expressed nondimensionally by dividing by radius of turn of attacker.

ANALYSIS

Geometric Considerations

A simplified analysis of the attack phase of an interception in which the fighter employs collision-course tactics has been given in reference 3. In this reference a simple geometric approach was employed. This method was considered justified by comparison with results obtained in more exact simulations of the problem. Most of the relations employed in this section of the present report follow the method of analysis used in reference 3. For completeness, a derivation of these relations is given herein.

The flight path assumed for the interceptor is shown in figure 1. In the attack, which is assumed to take place in a horizontal plane,

the target is detected by the radar of the fighter at the range R. In practice this distance R is not fixed but has a certain probability distribution. For the present purpose, however, a fixed average value will be assumed. After the target is detected, the fighter continues on a straight course for a distance l_1, which may include lag in the action of the fire-control system of the fighter and the time required for the fighter to roll. The fighter then enters a steady turn which is assumed to take place at constant speed. The fighter recovers from the turn and flies straight for a distance l_2 on a lead-collision course appropriate to the conditions of the problem. The missiles are then launched and travel the remaining distance l_3 to the collision point. No evasive action on the part of the target is considered.

For any given initial conditions some optimum heading ψ_c for the fighter exists which places the fighter on the desired lead-collision course. If the fighter is not initially on this desired course, the direction of turn required is determined by a comparison of the existing heading and the optimum heading. From the geometry of the problem and from the knowledge that the time required for the missiles to reach the collision point must equal the time required for the target to reach this point, the following relations may be derived with the aid of figure 1:

$$R \sin \theta = \left(l_2 + l_3\right)\sin \gamma + \operatorname{sgn}(\psi_c - \psi) r(\cos \psi - \cos \gamma) + l_1 \sin \psi$$

$$\frac{R \cos \theta - \left(l_2 + l_3\right)\cos \gamma - \operatorname{sgn}(\psi_c - \psi) r(\sin \gamma - \sin \psi) - l_1 \cos \psi}{V_T} =$$

$$\frac{\operatorname{sgn}(\psi_c - \psi) r(\gamma - \psi) + l_1 + l_2}{V_A} + \frac{l_3}{V_M}$$

where sgn denotes the algebraic sign of a quantity. The equations may be simplified somewhat by expressing all distances as ratios to the radius of turn of the attacker. Therefore, let

$$R^* = \frac{R}{r} \qquad l_1^* = \frac{l_1}{r}$$

and so forth. The equations then may be written

$$\left.\begin{aligned} R^* \sin\theta &= \left(l_2^* + l_3^*\right)\sin\gamma + \operatorname{sgn}(\psi_c - \psi)(\cos\psi - \cos\gamma) + l_1^* \sin\psi \\ R^* \cos\theta &= \frac{V_T}{V_A}\left[\operatorname{sgn}(\psi_c - \psi)(\gamma - \psi) + l_1^* + l_2^*\right] + \frac{V_T}{V_M} l_3^* + l_1^* \cos\psi + \\ &\quad \operatorname{sgn}(\psi_c - \psi)(\sin\gamma - \sin\psi) + \left(l_2^* + l_3^*\right)\cos\gamma \end{aligned}\right\} \quad (1)$$

An implicit formula for the optimum heading may be derived from these relations by setting $\psi = \gamma = \psi_c$:

$$R\cos\theta - K_c R\sin\theta = l_3\left(\frac{V_T}{V_M} - \frac{V_T}{V_A}\right) \quad (2)$$

where

$$K_c = \frac{V_T/V_A + \cos\psi_c}{\sin\psi_c}$$

The asterisks have been omitted from R and l_3 in this formula because the value of r, which may be canceled from the equations, does not enter a problem involving straight flight.

As explained in reference 1, certain conditions must be met for the attack to be successfully completed. First, the target must fall within the look angle of the radar of the fighter throughout the encounter. This relation is satisfied if

$$\psi - \theta \leqq \lambda_{max}$$

This relation has been applied only at the start of the attack because of the difficulty of checking this condition throughout the encounter. The look angle ordinarily decreases when the attacker starts a turn toward the target. Because the look angle may not decrease until this turn is started, however, a slight approximation is involved in applying

this formula at the start of the attack. A second condition to be met is that the fighter must have time to complete its turn and settle down on the direction of the lead-collision course before the desired range for missile firing is reached. The limiting combinations of variables for this condition to exist are known as maneuverability limits and may be derived from equations (1) by setting $l_2^* = 0$

$$\left.\begin{aligned} R^* \sin\theta &= l_3^* \sin\gamma + \operatorname{sgn}(\psi_c - \psi)(\cos\psi - \cos\gamma) + l_1^* \sin\psi \\ R^* \cos\theta &= \frac{V_T}{V_A}\left[\operatorname{sgn}(\psi_c - \psi)(\gamma - \psi) + l_1^*\right] + \frac{V_T}{V_M} l_3^* + l_1^* \cos\psi + \\ &\quad \operatorname{sgn}(\psi_c - \psi)(\sin\gamma - \sin\psi) + l_3^* \cos\psi \end{aligned}\right\} \quad (3)$$

In order that the fighter should not be exposed to the defensive armament of the target for an unduly long period, it is desirable that the fighter should not approach too closely the tail cone of the target. This condition, known as the vulnerability limit, may be derived from equations (1) by setting γ equal to a constant, the desired minimum approach angle. The following relation which provides an explicit solution for θ in terms of R^*, ψ, and γ may be derived from equations (1) by eliminating l_2^* between the two equations:

$$R^* \sin\theta = \frac{-K_2K_1 \pm \sqrt{R^{*2}\left(1 + K_1^2\right) - K_2^2}}{1 + K_1^2} \quad (4)$$

where

$$K_1 = \frac{(V_T/V_A) + \cos\gamma}{\sin\gamma}$$

and

$$K_2 = \frac{V_T}{V_A}\left[\operatorname{sgn}(\psi_c - \psi)(\gamma - \psi) + l_1^* - l_3^*\right] + \frac{V_T}{V_M} l_3^* + l_1^* \cos \psi +$$

$$\operatorname{sgn}(\psi_c - \psi)(\sin \gamma - \sin \psi) +$$

$$\left[\operatorname{sgn}(\psi_c - \psi)(\cos \gamma - \cos \psi) - l_1^* \sin \psi\right] K_1$$

If the analysis is to represent a monowing missile rather than a rocket-armed interceptor, the same relations may be employed with the exception that l_3^* is set equal to zero. In the preceding formulas, the quantity $(\gamma - \psi)$ must be less than 2π in order that the attacker should make less than a 360° turn during the attack. The term $\operatorname{sgn}(\psi_c - \psi)$ may become ambiguous when the values of ψ_c or ψ are large. In order for the term to yield the correct sign in all cases, the value of ψ should be measured in the range $\psi_c \pm 180^\circ$. For example, if ψ_c is 80° and ψ may be given as $+270^\circ$ or -90°, the value -90° should be inserted in the formula.

Graphical Method

A simple graphical or analog method of solution of the interception problem has been found convenient for an approximate solution of the problem and for visualization of various attack conditions. This method is illustrated in figure 2. In this method a paper tape is marked off to a convenient scale to represent the distance in miles traveled by the fighter. A similar tape is marked off at intervals corresponding to the distance traveled by the target in the time required for the fighter to travel 1 mile. A series of circular disks are constructed with radii corresponding to the radii of turn of the fighter at various values of normal acceleration. In order to represent the flight path corresponding to desired initial conditions, the zero of the fighter tape is placed at the initial point and its direction is taken as the initial heading of the fighter path. The disk is placed tangent to this path at the point at which the fighter starts to turn toward the target. The fighter tape is wrapped around the disk and extended over the path of the target until the numbers on the fighter and target tapes are equal. This condition then represents the geometric layout of a collision course. The example shown in figure 2 does not include the effect of missile firing. This effect may be accounted for, however, by causing the fighter and target

tapes to intersect at a point at which the number on the fighter tape exceeds the number on the target tape by a given value, rather than at a point with equal values of these numbers. The given difference represents the distance that the missile is ahead of the fighter at the time of impact. By suitable procedures, evasive action of the target or errors in the flight path of the fighter may be simulated. The method becomes inconvenient, however, if it is desired to take into account speed changes of the fighter.

Determination of Point for Effective Start of Constant-Radius Turn

The preceding methods of analysis have assumed that the fighter instantaneously enters a constant-radius turn, whereas in practice a finite time is required to reach this condition. The point at which the fighter may be considered to enter a constant-radius turn depends upon both the rate of roll and the manner in which the normal acceleration is applied. During the roll some lateral displacement of the flight path will occur before a steady angle of bank is reached. Inasmuch as one objective of this analysis is to study the effects of rate of roll on the interception problem, it is desired to establish approximately the point in the roll at which the effective start of a constant-g turn occurs for various manners of coordination of the normal acceleration with the roll angle. For this analysis the angle of bank is assumed to vary, as shown in figure 3(a), from zero to a steady value ϕ_o in the time T_o, in accordance with the formula:

$$\phi = \phi_o \sin^2 \frac{\pi t}{2T_o} \tag{5}$$

This formula is arbitrarily chosen for convenience inasmuch as variations in piloting technique would result in different forms for the variation of bank angle. Three possible types of variation of normal acceleration which may be considered to represent extremes likely to be encountered in practice are shown in figure 3(b). These variations are as follows:

Case 1. Pulling up to the value of normal acceleration required in the steady turn before starting the roll

Case 2. Increasing the normal acceleration as a function of angle of bank as required for a coordinated turn entry (vertical component of acceleration equals 1 g)

Case 3. Maintaining a normal acceleration of 1 g during the roll, then pulling up to the value required in a steady turn at the time the roll is completed

For these three conditions the variations of the lateral component of acceleration, given by the formula $a_l = a_n \sin \phi$, have been plotted for various values of the final normal acceleration. These variations are illustrated for a 2g turn in figure 3(c). The effective start of the turn was assumed to occur at the point at which the steady final acceleration would have to be applied to give the same lateral velocity at time T_o as that obtained by integrating the lateral acceleration. Thus, if T_1 is the time to the effective start of the turn,

$$\frac{T_1}{T_o} = 1 - \frac{\int_0^{T_o} a_l \, dt}{a_{l,max} T_o}$$

The path obtained by drawing a curve of constant radius tangent to the original line of flight at time T_1 is not exactly equivalent to the true path of the fighter inasmuch as the turn following a gradual buildup of lateral acceleration is displaced laterally from the original line of flight. This difference is of small importance in problems involving high-speed aircraft, however. Thus, in a 4g turn entered in 2 seconds the lateral displacement of the true path from the assumed path would be 26.8 feet. This distance is small compared with other dimensions involved in the maneuver. For example, the distance traveled during the turn entry would be 1,940 feet at a Mach number of 1.

DISCUSSION

Variables Influencing Success of Attack

In order to appreciate the interception problems under discussion, a visualization of the geometry of some of the attack situations is desirable. Such a visualization for a wide variety of cases may be obtained by the analog method discussed previously. The effects of certain variables to be discussed are illustrated for a few cases in figure 4. In this and in succeeding figures, speed of the airplanes is expressed as Mach number based on a speed of sound of 971 feet per second (corresponding to standard atmospheric conditions between 35,500 and 80,000 feet). Inasmuch as the geometry of the attack situations is a function of true speed, the Mach number given should be interpreted as a measure of true speed. A successful attack is illustrated in

figure 4(a). In this case, the attacker has been vectored by ground control to a point at which it is able to pick up and lock on the target with its own radar. Though the initial heading of the attacker is not the optimum, it is able, by entering a turn, to reach a collision course in time to launch its missiles. Furthermore, the other conditions described in the section "Analysis" for a successful attack are met. That is, the look angles remain reasonable throughout the encounter, and the angle of the final collision course is not too close to the tail cone of the target.

The effect of increasing the radius of turn of the fighter (by use of a lower-g turn) while keeping other factors constant is shown in figure 4(b). The increased-radius turn results in slightly greater target penetration and a smaller angle off the tail cone of the target, but the attack is still successful. A further increase in radius of turn, however, as shown in figure 4(c), allows the target to pass the attacker before a collision course can be established. In this example the initial conditions lie outside the maneuverability limits (eqs. (3)). If the attacker is assumed to have a speed advantage, the attack could be continued only as a tail chase or as a new encounter with large target penetration. In many cases of this type, the look angle of the radar would be exceeded and dependence on ground vectoring would be renewed. This encounter is therefore considered unsuccessful.

The effect of delaying the initial turn is shown in figure 4(d). Such a delay might result, in part, from time required for the attacker to roll. In the case shown, the attack is still successful but results in slightly greater target penetration. Further large increases in the delay time would result in an unsuccessful attack. The effect of differences in time to roll out of the turn have not been considered in subsequent calculations because the roll out of the turn could be started before reaching the final collision-course path and could be performed gradually with very little effect on the geometry of the problem.

From the foregoing considerations and from the formulas presented in the section on "Analysis," factors governing the success of an attack may be seen to be the ratio of radar range to radius of turn of the attacker, the ratio of target speed to attacker speed, the initial position and heading of the attacker with respect to the target path, the allowable angle off the tail cone of the target, the time required to enter a turn following radar acquisition, and the range at which the missiles must be released in order for the attacker to break away and evade the explosion or debris resulting from a hit. In the present analysis, this range has been assumed to be short as compared with other dimensions of the problem, a condition applicable with conventional rockets having low explosive energy. If weapons of much greater explosive energy were considered, this factor would require further consideration.

Effect of Rolling Performance on Success of Attack

Effect of roll rate and acceleration on time to bank.- Roll requirements in the present military specification for handling qualities of fighter airplanes in the high-speed condition are expressed in terms of the time to roll through 100° (ref. 4). This method of stating the requirements has the advantages of providing a convenient and reproducible measuring technique and of combining the influences of maximum rolling acceleration and maximum rolling velocity in about the same way that they enter in actual tactical maneuvers. In order to relate the specified performance to problems of airplane design, however, it is desirable to relate the time to roll through a given angle to the maximum rolling acceleration and maximum rolling velocity produced by the ailerons. Figure 5 shows this relation. The curves of this figure were calculated by the method described in reference 1, which is based on the assumption that the rolling response of the airplane may be represented as that of a system of one degree of freedom with inertia and damping. The values of the time constant in roll τ are also shown $\left(\tau = \frac{-4I_X}{C_{l_p}\rho V b^2 S}\right)$. The curves of figure 5 show that large changes in maximum rolling acceleration and maximum rolling velocity are required to produce relatively small changes in the time to roll through 100°. For example, with a typical value of τ of 0.6 second, an increase of aileron effectiveness of 60 percent would be required to reduce the time to roll through 100° from 1.0 second to 0.75 second.

Point of effective start of constant-radius turn.- When the attacking airplane detects a target and rolls into a turn to make an attack, the important delay is the time required to start curving the flight path rather than the time required to roll. This delay is a function not only of rolling performance but also of the manner of coordinating normal acceleration with bank angle during the turn entry. By the method described in the section on "Analysis," the ratio of the time to the effective start of a constant-radius turn to the time required to reach a steady bank angle has been calculated for three types of variation of normal acceleration with bank angle. These results are shown in figure 6. This figure shows a marked decrease in the time to enter a turn when the normal acceleration is applied at the start of the maneuver rather than after reaching a steady bank angle. The case of a coordinated turn entry gives intermediate values of delay. The case of the coordinated turn entry has been used in the subsequent calculations as an average representation of pilot technique for purposes of studying the effects of rolling performance. The results shown in figure 6 indicate, however, that the normal acceleration should be applied as rapidly as possible when rolling into a turn. When the small reductions in time to bank accomplished by large increases in aileron power are considered,

the use of correct piloting technique to reduce the delay time appears particularly important.

Effect of rolling performance and acceleration capability on success of attack.- By the methods described in the section on "Analysis," the limiting combinations of variables required for a successful attack may be calculated. These combinations of variables, called vectoring limits in reference 3, are expressed herein in terms of the initial heading of the fighter ψ and the angle between the target flight path and the line of sight between the target and the attacker θ (see fig. 1). For a given value of the radar range R, these variables completely define the initial attack situation. The effect of any design variable on the success of the attack may be judged by its effect in broadening or narrowing the region in a plot of ψ against θ for which successful attacks are possible.

The various boundaries limiting the success of the attack are described in the section on "Analysis" as look-angle limits, maneuverability limits, and vulnerability limits. Although the look-angle limits may be calculated very simply, the other limits require the solution of transcendental equations. These equations were solved numerically by a method of successive approximations using a card-programed digital computer.

Because of the large number of variables involved in the attack equations, a large number of solutions would be required to provide a survey of the effects of all the variables. A number of such solutions are presented in reference 3. In the present analysis, a set of results more accurate than could be obtained by reading values from the curves of reference 3 was desired. For this reason, solutions were carried out for a single set of conditions given in table I. The Mach number of the target was taken as 1.0 and that of the attacker as 1.5. The variables considered were the normal-acceleration capability of the attacker (2 to 6g) and the time (or distance l_1) required to pull into the initial turn.

Since the method of computing the times required to pull into the initial turn is somewhat arbitrary, it is now described. These times were based on three conditions, namely: instantaneous turn entry, turn entry with time to roll corresponding to the requirement of 1 second to roll through 100°, and turn entry with time to roll corresponding to a much reduced requirement of 4 seconds to roll through 100°. The corresponding rolling performance, determined from figure 5 and from the methods of reference 1, is as given in the following table (τ = 1.2 sec):

Time to roll through 100°, sec	p_{max}, radians/sec	$\dot{p}_{max}$, radians/sec^2	Time to roll to and stop at 90° bank, T_o, sec
0	∞	∞	0
1	5.42	4.51	1.20
4	.63	.52	4.10

Inasmuch as the angles of bank corresponding to the values of steady acceleration of 2 to 6g are somewhat less than 90°, the times to reach these angles were reduced from that required to roll 90°. This reduction was carried out by an approximate method because the use of the single-degree-of-freedom calculations, such as those used to determine the time to roll to and stop at 90° bank, was considered more time-consuming than necessary. The time history of bank angle for the 90° bank case was assumed to be given by the sine-squared variation used in equation (5) with the value of T_o given in the preceding table. The time histories of bank angle for the cases of smaller bank angles were obtained by assuming the time history in each case to be identical with that of the 90° bank case up to one-half of the final bank angle. The time to reach this point was then doubled to obtain the time to reach the final bank angle. This procedure, in effect, assumes that the initial rolling acceleration remains the same in each case. The times to the effective start of the steady turns were then determined by multiplying these times by the factor, determined from figure 6, to take into account the buildup of acceleration in a coordinated turn entry. The resulting times and distances to pull into the turn are given in the following table:

a_n, g units	Angle of bank, deg	Time to roll, sec	Time to enter turn, T_1, sec	Distance to enter turn at M = 1.5, miles
T_{100} = 1 sec				
2	60.0	0.94	0.552	0.152
3	70.5	1.03	.662	.183
4	75.5	1.08	.730	.202
5	78.5	1.10	.776	.212
6	80.4	1.12	.810	.223
T_{100} = 4 sec				
2	60.0	3.21	1.89	0.522
3	70.5	3.53	2.26	.624
4	75.5	3.68	2.49	.688
5	78.5	3.76	2.64	.730
6	80.4	3.82	2.76	.763

Vectoring limits for the cases calculated are given in figure 7. This figure shows the look-angle limits, maneuverability limits, and vulnerability limits for all the conditions of normal acceleration and rolling performance. For each condition, the region enclosed by the limiting boundaries is the region of successful attacks. The boundaries are antisymmetrical about the axes of ψ and θ. For this reason, the curves on one side of the axes have been cut off in order to permit a larger scale for the remainder of the figure. The look-angle limits are shown only for $\lambda_{max} = 90^{\circ}$. For any other value of λ_{max}, however, the look-angle limits would be straight 45° lines passing through the value of λ_{max} on the ψ-axis.

Discussion of factors influencing choice of rolling performance.- The data of figure 7 show that the variations in normal-acceleration capability, over the range presented, have a much greater influence on the success of the attacks than the variations in rolling characteristics. The case of very low rolling performance (100° in 4 seconds) was chosen primarily to produce enough change in the vectoring limits to be clearly visible in figure 7. Such low rolling performance in a fighter would be entirely unsatisfactory from the pilots' standpoint.

The choice of rolling performance to be provided in a fighter airplane is difficult because many desirable features may need to be compromised to satisfy the pilots' preference for high rolling performance. For example, the problem of roll coupling may require increases in vertical-tail size, structural beef-up, or the provision of automatic control systems. Conflicting requirements may exist between ailerons and high-lift devices. Provision of high rolling performance at high values of dynamic pressure may require special types of ailerons, such as spoilers, which complicate the lateral-control system and which may be less satisfactory than other designs in flight regimes such as landing approach or spin recovery. For this reason, the actual tactical benefits to be derived from high rolling performance should be closely examined.

For the collision-course attack situation considered herein, it is evident from the vectoring limits plotted in figure 7 that if the rolling performance must be reduced as a result of design problems such as roll coupling, conflict with high-lift devices, and so forth, only a slight reduction in the probability of successful attacks is to be expected. On the other hand, any aerodynamic feature that results in a substantial increase in normal-acceleration capability has a marked beneficial effect on the success of attacks. Every effort, therefore, should be made to improve the normal-acceleration capability of interceptors.

The success of attacks has been shown to increase with normal-acceleration capability and with rolling performance. Increasing the rolling performance, however, usually requires some increase in structural weight which, if other factors are held constant, reduces the

normal-acceleration capability. For this restricted situation, then, the determination of an optimum rolling performance should be possible. An attempt has been made to carry out such an analysis for the conditions considered in figure 7. This analysis applies only at high altitudes where the maximum normal acceleration is limited by lift coefficient. As shown in figure 7, the radar look angle becomes an important factor in determining the success of attacks at the higher values of normal acceleration. The analysis is therefore applicable at values of normal acceleration below about 4g, where the normal acceleration and rolling performance are the factors primarily influencing the success of attacks.

In order to optimalize the rolling performance, a measure of the success of the attack in terms of the vectoring limits is required. As shown in figure 7, the changes in vectoring limits caused by changes in the variables a_n and T_{100} are fairly uniform throughout the range of values of ψ and θ (except near the values corresponding to the ideal collision course, where no maneuvering is required to intercept the target). For this reason, increments of θ at $\psi = 0$ have been selected as representative of the changes caused by roll performance and acceleration capability. Since the weight is assumed to vary as a function of roll performance, the optimum aileron power may be obtained by satisfying the relation

$$\frac{d\theta}{dw} = 0 \tag{6}$$

The increments of θ are attributed to changes in aileron power, as measured by the time to roll through 100° T_{100} and to changes in maximum normal acceleration a_n. Equation (6) may therefore be expressed:

$$\frac{\partial\theta}{\partial T_{100}} \frac{dT_{100}}{dw} + \frac{\partial\theta}{\partial a_n} \frac{da_n}{dw} = 0 \tag{7}$$

By dividing the denominator by the weight, fractional rather than absolute changes in weight are considered. This procedure is used to make the results more generally applicable to airplanes of various weights. Equation (7) then becomes

$$\frac{\partial\theta}{\partial T_{100}} \frac{dT_{100}}{dw/w} + \frac{\partial\theta}{\partial a_n} \frac{da_n}{dw/w} = 0$$

The methods for obtaining the various terms in this expression are now discussed. First, consider the terms $\partial\theta/\partial T_{100}$ and $\partial\theta/\partial a_n$. The increments of θ at $\psi = 0$ were determined from the data of figure 7 and plotted as functions of T_{100} and of a_n, and the slopes were determined graphically. Though figure 7 is plotted to a scale too small to allow incremental changes in θ to be measured accurately, the original digital-computer solutions provide adequate accuracy. The slope $\partial\theta/\partial T_{100}$ was found to remain fairly constant at values of normal acceleration of 3g and greater. This value was taken as -1.8° per second. The slope $\partial\theta/\partial a_n$ was taken as 15.1° per g.

The term $\frac{da_n}{dw/w}$, the variation of maximum normal acceleration with fractional increase in gross weight, is simply equal to $-a_{n,max}$ at altitudes for which the maximum normal acceleration is limited by lift coefficient. A value of 3g was assumed for $a_{n,max}$.

Finally, the term $\frac{dT_{100}}{dw/w}$ is considered. In general, improvement in rolling performance is sought by increasing the rolling moment applied to the airplane. This change may be accomplished by increasing the aileron size or deflection range, by adding auxiliary control surfaces such as spoilers, or by stiffening the wing structure to avoid adverse aeroelastic effects. The increased rolling moment does not change the time constant in roll τ. The weight increment due to the change, however, is likely to be added in the wings and therefore increases the moment of inertia in roll. The effect of increased inertia is to increase the time constant τ without changing the maximum rolling velocity. A change in wing stiffness might also affect the damping in roll and thereby change τ, but this effect is neglected in the subsequent analysis.

In order to determine $\frac{dT_{100}}{dw/w}$, the effects of the increased rolling moment and the increased time constant are considered separately and added. This procedure is expressed by the following formula:

$$\frac{dT_{100}}{dw/w} = \left(\frac{\partial T_{100}}{\partial p_{max}} \frac{dp_{max}}{dw/w}\right)_{\tau} + \left(\frac{\partial T_{100}}{\partial \tau} \frac{d\tau}{dw/w}\right)_{p_{max}} \tag{8}$$

The subscripts to the terms in parentheses indicate the quantities held constant. The second term of this formula is further expanded as follows:

$$\left(\frac{\partial T_{100}}{\partial \tau}\,\frac{d\tau}{dw/w}\right)_{p_{max}} = \left(\frac{\partial T_{100}}{\partial \dot{p}_{max}}\,\frac{\partial \dot{p}_{max}}{\partial \tau}\,\frac{d\tau}{dw/w}\right)_{p_{max}} \tag{9}$$

The data of figure 5 are used to evaluate the terms in these formulas. Inasmuch as this figure was calculated on the assumption that the rolling response is represented by a single-degree-of-freedom system, the following relation holds:

$$\dot{p}_{max} = \frac{p_{max}}{\tau}$$

hence,

$$\left(\frac{\partial \dot{p}_{max}}{\partial \tau}\right)_{p_{max}} = \frac{-p_{max}}{\tau^2} = \frac{-\dot{p}_{max}}{\tau}$$

If this expression is substituted in equation (9) and in turn in equation (8), the resulting expression may be placed in the following form which is convenient for numerical evaluation:

$$\frac{dT_{100}}{dw/w} = \left(\frac{\partial T_{100}}{\partial p_{max}}\,p_{max}\,\frac{dp_{max}/p_{max}}{dw/w}\right)_{\tau} - \left(\frac{\partial T_{100}}{\partial \dot{p}_{max}}\,\dot{p}_{max}\,\frac{d\tau/\tau}{dw/w}\right)_{p_{max}}$$

In evaluating the first term, the variations of T_{100} with p_{max} for various constant values of τ were cross-plotted from figure 5. The slopes $\partial T_{100}/\partial p_{max}$ and the corresponding values of p_{max} were read from these cross plots. The quantity $\frac{dp_{max}/p_{max}}{dw/w}$, which expresses the fractional increase in rolling velocity per fractional increase in gross weight, is dependent on the individual airplane design. A range of values is subsequently assumed for this parameter. The use of a nondimensional form for this parameter makes it proportional to the fractional increase in rolling moment, which as mentioned previously, is the primary variable used to produce an increase in rolling performance.

In evaluating the second term in this expression, the variations of T_{100} with $\dot{p}_{max}$ for constant values of p_{max} were cross-plotted from figure 5, and the slopes $\left(\frac{\partial T_{100}}{\partial \dot{p}_{max}}\right)_{p_{max}}$ and the corresponding values of $\dot{p}_{max}$ were read from the cross plots. The quantity $\frac{d\tau/\tau}{dw/w}$, the fractional increase in τ per fractional increase in gross weight, is proportional to the fractional increase in moment of inertia in roll per fractional increase in gross weight. Two values have been assumed for this parameter, 0 and 10. The value of 0 corresponds to the case in which all the added weight is in the fuselage, as might occur if the aileron actuator power were increased. The value of 10 corresponds to a case in which all the added weight is near the wing tips, as might occur with increased aileron size, increase in wing stiffness, and so forth. Detailed knowledge of the airplane design would be required to determine the actual value to be used in a particular case. The values assumed, however, probably bracket the values likely to be encountered in practice.

The results of this analysis are shown in figure 8 as plots of the optimum time to roll through 100° as a function of $\frac{dp_{max}/p_{max}}{dw/w}$ for three values of τ. Figure 8(a) shows the case for $\frac{d\tau/\tau}{dw/w} = 0$ and figure 8(b) shows the case for $\frac{d\tau/\tau}{dw/w} = 10$. The interpretation of these figures is as follows: If an increment of rolling velocity is costly in terms of weight $\left(\text{low value of } \frac{dp_{max}/p_{max}}{dw/w}\right)$, the optimum rolling performance is low, whereas if an increment of rolling velocity is obtainable with little weight penalty $\left(\text{high value of } \frac{dp_{max}/p_{max}}{dw/w}\right)$, the optimum rolling performance is high. A low value of τ results in a greater optimum rolling performance. If the weight increase results in an increase in moment of inertia in roll, the optimum rolling performance is decreased somewhat.

The quantity $\frac{dp_{max}/p_{max}}{dw/w}$ is difficult to estimate without a detailed knowledge of an airplane design. If it is assumed that an increment of

maximum rolling velocity would require a proportional increase in the weight attributable to the aileron control system, a value of about 50 (50 percent increase in rolling velocity for 1 percent increase in gross weight) would seem reasonable for current designs. This value would generally place the optimum rolling performance higher than the requirement of 1 second to roll through 100°.

The weight penalty involved in increasing rolling performance at high altitude actually may not provide a valid measure of the price to be paid for increased rolling performance. In fact, increased rolling velocity at high altitude might be possible with little or no increase in weight, because the structure, designed for higher loading conditions at low altitude, would already be strong enough to withstand increased aileron loads. In practice, the aileron loads become critical at low altitude, where increased wing stiffness must be provided to avoid aileron reversal. At low altitude, however, the increased weight does not reduce the normal-acceleration capability, which is fixed at the specified limit load factor. The increased weight would reduce the acceleration capability at high altitude. Under these conditions, the foregoing analysis would not apply. Some relative importance would have to be assigned to the success of attacks at low and high altitude in order to arrive at a decision as to the optimum rolling performance.

Further consideration would have to be given to the effect of increased weight on range, payload, or other performance items in order to evaluate fully the effect of an increase in rolling ability. These factors are mentioned simply to emphasize further that a limited analysis such as that described herein cannot give a complete answer to the problem of optimum aileron effectiveness. In view of the complicated nature of the problem and the need for knowledge of the design considerations of an individual airplane, the results of the foregoing analysis should not be applied quantitatively. The method used, however, may serve as a guide for similar analyses of problems involving tactical considerations.

In the preceding analysis, no consideration has been given to the effects of evasive action of the target. For collision-course attacks in which a side approach is used, little rolling on the part of the attacker would be required to counter target maneuvers. In tail-chase approaches, the requirements would be similar to those for pursuit-type attacks discussed in reference 1. This type of approach, however, is not likely to be used because it fails to take advantage of the benefits of the collision-course attack in reducing the effectiveness of tail defense weapons of the target. The case of a head-on approach requires further analysis. Preliminary considerations indicate, however, that the relative importance of rolling performance and normal-acceleration capability for this case would be similar to that determined by neglecting evasive action by the target.

Effect of Interceptor Speed and Radar Range on Success of Attack

The preceding analysis has shown the relative importance of roll performance and normal-acceleration capability on the success of attacks. The equations presented in the section on "Analysis" show, however, that interceptor speed and radar range are also important variables in determining the success of attacks. For this reason, limited analyses have been made to show some of the effects of these variables.

Effect of interceptor speed.- A complete analysis of the effect of a variable such as interceptor speed would require the calculation of vectoring limits, such as those given in figure 7, for a range of values of interceptor speed. In order to simplify the calculations, the present analysis has been restricted to the case of head-on attacks ($\psi = 0$) with various values of lateral displacement (sometimes called offset) of the flight paths of the attacker and target. The effect of missile firing was omitted from these calculations because, for the short-range missiles assumed previously, the effect of the missiles on the geometry of the interceptions was small. The minimum angle of the attacker from the target path was again assumed to be 30°. The maximum lateral displacement from which an attack can be successfully completed is shown as a function of attacker Mach number for a typical case in figure 9. The conditions assumed are as given in table II. The curves were calculated with the aid of equations (3) and (4).

The results show that the allowable lateral displacement increases to a maximum at a particular value of attacker speed and decreases with further increase in speed. The optimum speed is generally that at which a transition occurs from maneuvers limited by the maximum usable normal-force coefficient to those limited by the maximum allowable acceleration. In other words, the optimum speed is that corresponding to the upper left-hand corner of the V-g diagram. This condition might not always apply, as shown by the curve for $C_{N,max} = 1.0$, for which a slightly higher speed is seen to be beneficial. The peak of the curve of lateral displacement as a function of attacker Mach number for the case of constant normal acceleration occurs at progressively higher values of Mach number as the radar range is increased. Also, the speed corresponding to the upper left-hand corner of the V-g diagram is reduced at low altitude. In cases of long radar range or low altitude, therefore, the maximum point of the curve of lateral displacement against Mach number is likely to occur at a Mach number higher than the speed corresponding to the upper left-hand corner of the V-g diagram. Unfortunately, because of the complication of the equations, no simple expression can be derived for the speed at which this maximum point occurs. A number of solutions of equation (4) would be required to plot the curve for each case of interest as was done in preparing figure 9.

In order to avoid long exposure to the defensive armament of the target and also to avoid large look angles during the latter stages of the attack, a reasonable margin of speed of the attacker over the target would appear desirable. Therefore, in the absence of a complete analysis of the optimum attack speed in a head-on attack, a reasonable rule appears to be to make the attack at a speed corresponding to the upper left-hand corner of the V-g diagram unless this speed is less than the target speed, in which case a speed higher than the target speed should be used. If the altitude is so high that the speed corresponding to the upper left-hand corner of the V-g diagram cannot be reached, the attack should be made at the highest speed possible. These calculations were made on the assumption of constant attacker speed. If slowdown occurred during the attack, approximate compensation for this variation could be made by starting the attack at a somewhat higher speed, so that the average speed during the attack would correspond to the calculated value.

The foregoing example, as mentioned previously, is limited to the case of head-on attacks. The optimum attack speeds would not be expected to differ greatly for small deviations from the head-on attack situation. For the case of arbitrary initial heading, however, the solution is much more complicated. The optimum attack speed would be different for paths displaced to the left or right of the desired collision-course path. Further investigation is required to study this general problem.

Effect of radar range.- Increasing the radar range of the attacker is always beneficial in that it increases the area from which successful attacks are possible. An optimum radar range cannot be determined, therefore, without considering adverse effects of a larger radar on the speed or range of the interceptor. These considerations are beyond the scope of this report. A simple example can be given, however, to show how the radar range should increase with interceptor speed in order to allow runs requiring geometrically similar maneuvers on the part of the interceptor. The ability to perform such similar runs would seem desirable in order to take full advantage of increased speed capabilities of an interceptor. An increase in speed alone, without an increase in radar range, is shown in figure 9 to be undesirable because the region for initiation of successful head-on attacks at given values of normal acceleration and radar range decreases rapidly with increasing interceptor speed.

A typical attack situation in which the interceptor is initially in a somewhat unfavorable position is shown in figure 10. The required ratio of radar range to radius of turn of the attacker is plotted as a function of the ratio of target speed to attacker speed. The curve has the form

$$\frac{R}{r} = C_1 \frac{V_T}{V_A} + C_2$$

Since r is proportional to V_A^2, the variation of required radar range with V_A has the form

$$R \propto C_1 V_T V_A + C_2 V_A^2 \tag{10}$$

Thus the radar range required to make an attack of this type varies somewhere between the first and second power of the interceptor speed. Although this simple form of the equations holds only when the initial point of the attack is on the projected flight path of the target, the actual variation for other initial conditions tends to have a similar form. The linear dimensions of the region from which successful attacks requiring geometrically similar maneuvers of the attacker can be started vary as the square of the attacker speed. Increased attacker speed is therefore highly beneficial if it is accompanied by increased radar range to the extent indicated by equation (10).

CONCLUDING REMARKS

In the analysis of this report, an attempt has been made to determine the relative importance of rolling performance and certain other factors in the design of an interceptor which uses collision-course tactics. A graphical method is presented for simple visualization of attack situations.

By means of diagrams showing vectoring limits, that is, the ranges of interceptor position and heading from which attacks may be successfully completed, the relative importance of rolling performance and normal-acceleration capability in determining the success of attacks is illustrated. In order to determine the optimum rolling performance, an attempt is made to balance the adverse effects of the weight penalty due to the ailerons against the benefits due to increased rolling performance. This analysis indicates that a high rolling performance is most favorable. This analysis, however, neglects many practical considerations which may make the provision of high rolling effectiveness difficult. The vectoring limits indicate that the reduction in success of attacks due to reduced rolling performance (within limits generally acceptable from the pilots' standpoint) is very small, whereas the advantage that may be gained by substantially increasing the normal-acceleration capability is large.

The analysis also indicates important effects of interceptor speed and radar range on the success of attacks. The optimum speed for initiation of a head-on attack is often that corresponding to the upper left-hand corner of the V-g diagram. In these cases, increasing speed beyond

this point for given values of normal acceleration and radar range rapidly decreases the width of the region from which successful attacks can be initiated. On the other hand, if the radar range is increased with a variation somewhere between the first and second power of the interceptor speed, the linear dimensions of the region from which successful attacks can be initiated increase as the square of the interceptor speed.

Langley Aeronautical Laboratory,
National Advisory Committee for Aeronautics,
Langley Field, Va., May 16, 1958.

REFERENCES

1. Adams, James J.: Flight and Analytical Study of Roll Requirements of a Fighter Airplane. NACA RM L56F12a, 1956.

2. Anon.: Navy Intercept Project. Quart. Eng. Rep. No. 26, vol. 1, (Contract NOa(s)-10413), Bell Telephone Labs., Inc. (for Western Electric Co., Inc.), 1956.

3. Prim, R. C.: Approximate Interceptor Vectoring Limit Computation. Appendix B, Navy Intercept Project. Quart. Eng. Rep. No. 21 (Contract NOa(s)-10413), Bell Telephone Labs., Inc. (for Western Electric Co., Inc.), 1954, pp. A9-A14, A70-A103.

4. Anon.: Flying Qualities of Piloted Airplanes. Military Specification MIL-F-8785(ASG), Sept. 1, 1954; Amendment-1, Oct. 19, 1954.

TABLE I

CONDITIONS FOR VECTORING-LIMIT CALCULATIONS

Attacker Mach number	1.5
Target Mach number	1.0
Missile Mach number (average)	2.5
Missile firing range, l_3, miles	0.690
Radar range, R, miles	12
Minimum angle from target path (for vulnerability-limit calculation), deg	30

(hence $\gamma = \frac{5\pi}{6}$ radians)

TABLE II

CONDITIONS FOR CALCULATION OF LATERAL DISPLACEMENT

OF FLIGHT PATHS IN HEAD-ON ATTACKS

Target Mach number	1.0
Radar range, R, miles	6
Maximum normal acceleration of attacker, g units	6
Attacker wing loading, lb/sq ft	70
Altitude, ft	35,000
l_1, l_3	0
Minimum angle from target path (for vulnerability-limit calculation), deg	30

(hence $\gamma = \frac{5\pi}{6}$ radians)

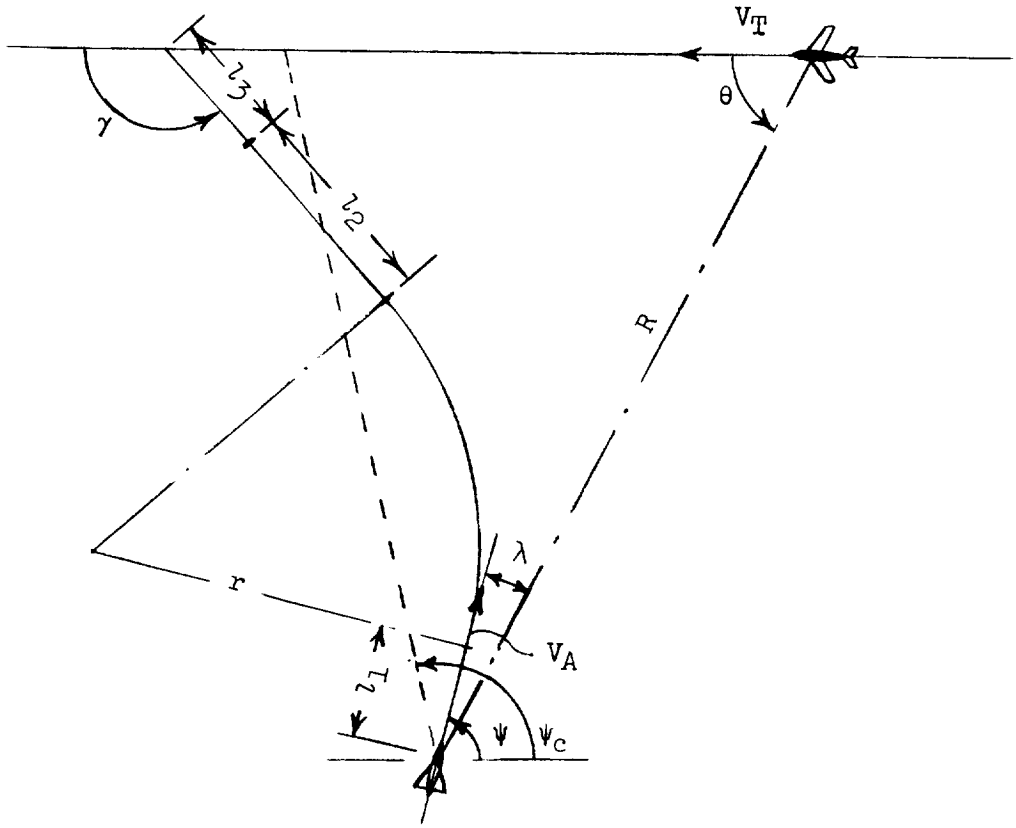

Figure 1.- Geometric characteristics of interceptor path.

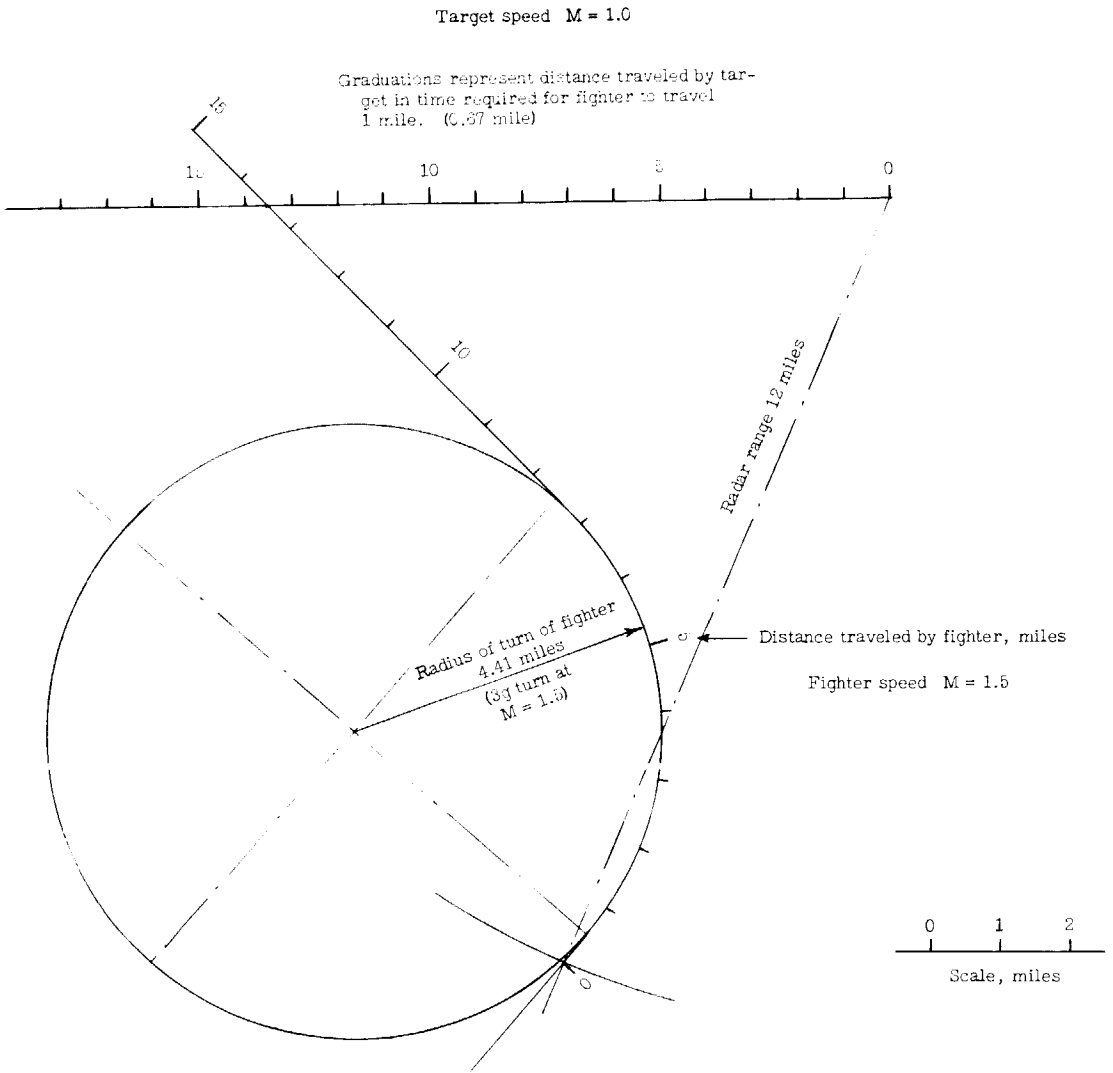

Figure 2.- Illustration of analog method for determining geometry of interception.

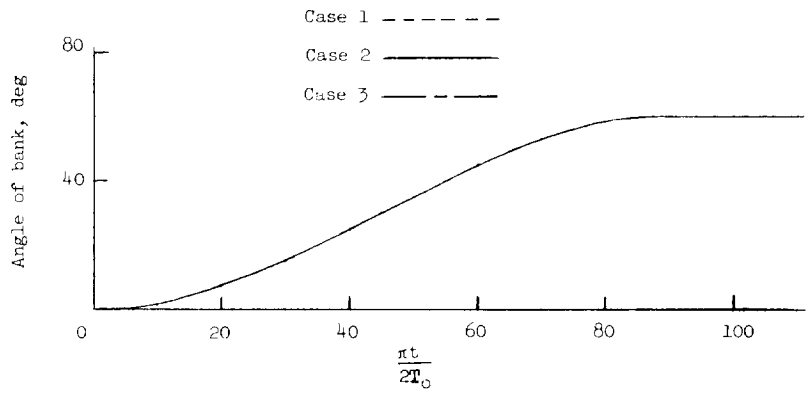

(a) Angle of bank.

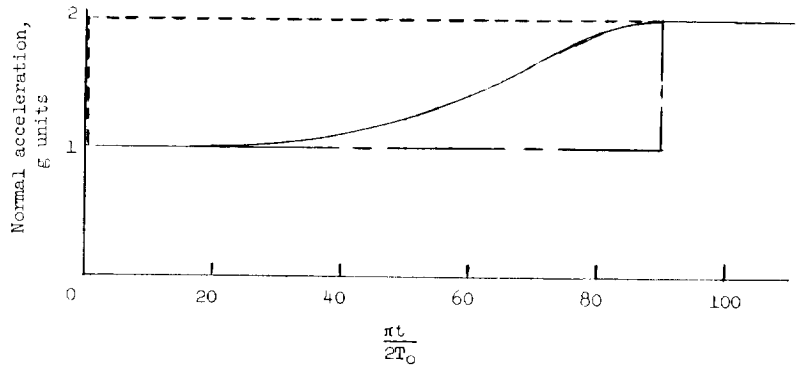

(b) Normal acceleration.

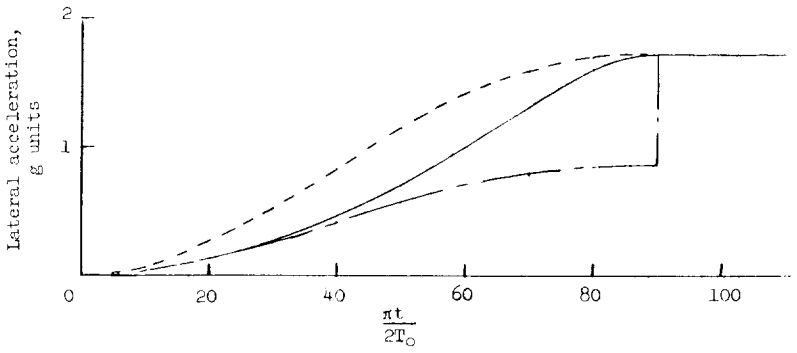

(c) Lateral acceleration.

Figure 3.- Variations of angle of bank, normal acceleration, and lateral acceleration with time in 2g turn entry for three types of variation of normal acceleration with bank angle.

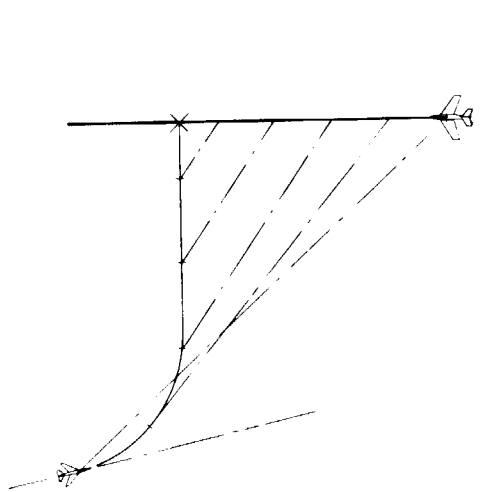

(a) 4g.

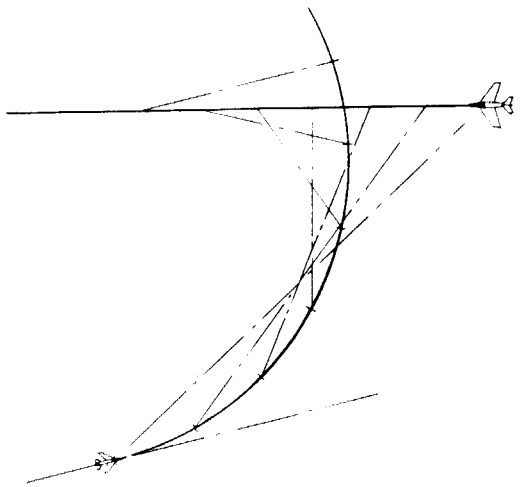

(c) 2g.

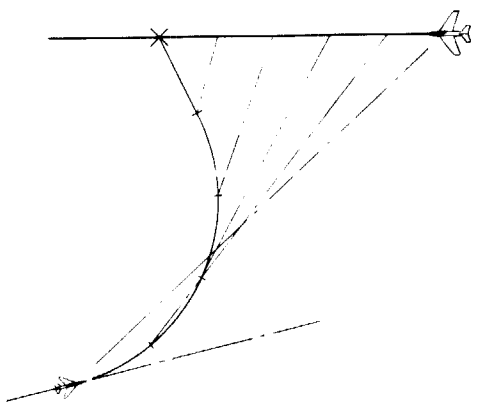

(b) 3g.

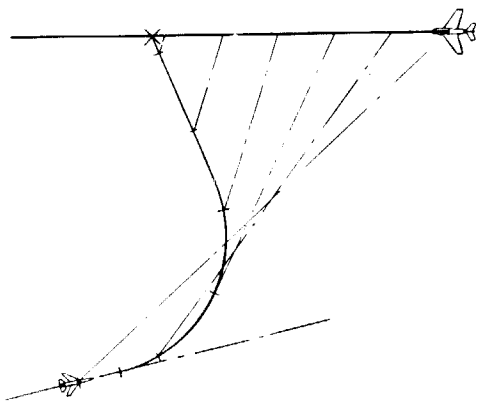

(d) 4g, 3.6 second delay.

Figure 4.- Illustration of geometry of attack situations. Target M = 1.0; attacker M = 1.5; radar range = 12 miles. Line of sight indicated at 2-mile intervals along path of attacker.

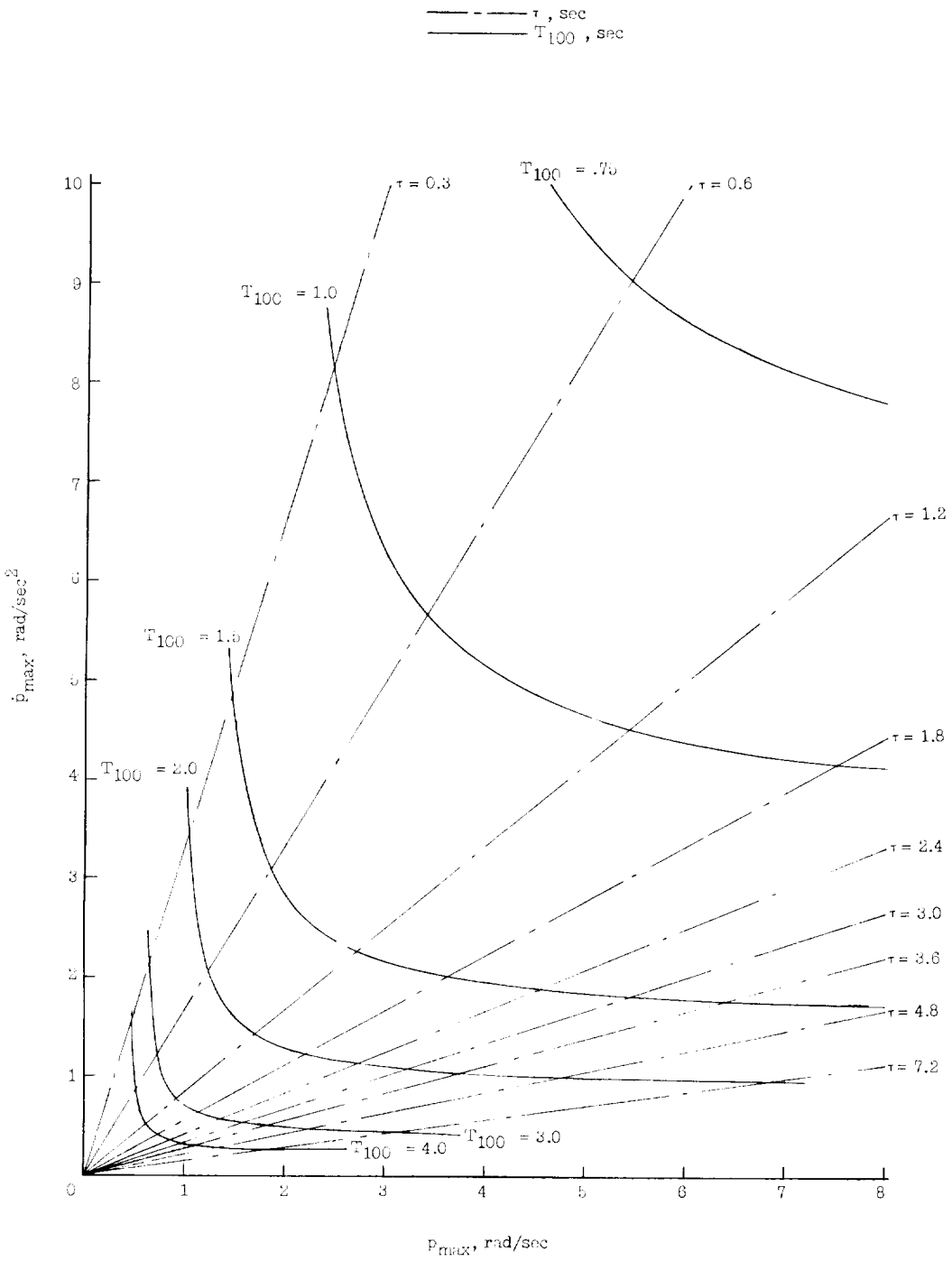

Figure 5.- Relation between time to roll through a bank angle of 100° and values of maximum rolling velocity and maximum rolling acceleration. Values of time constant in roll τ are also shown.

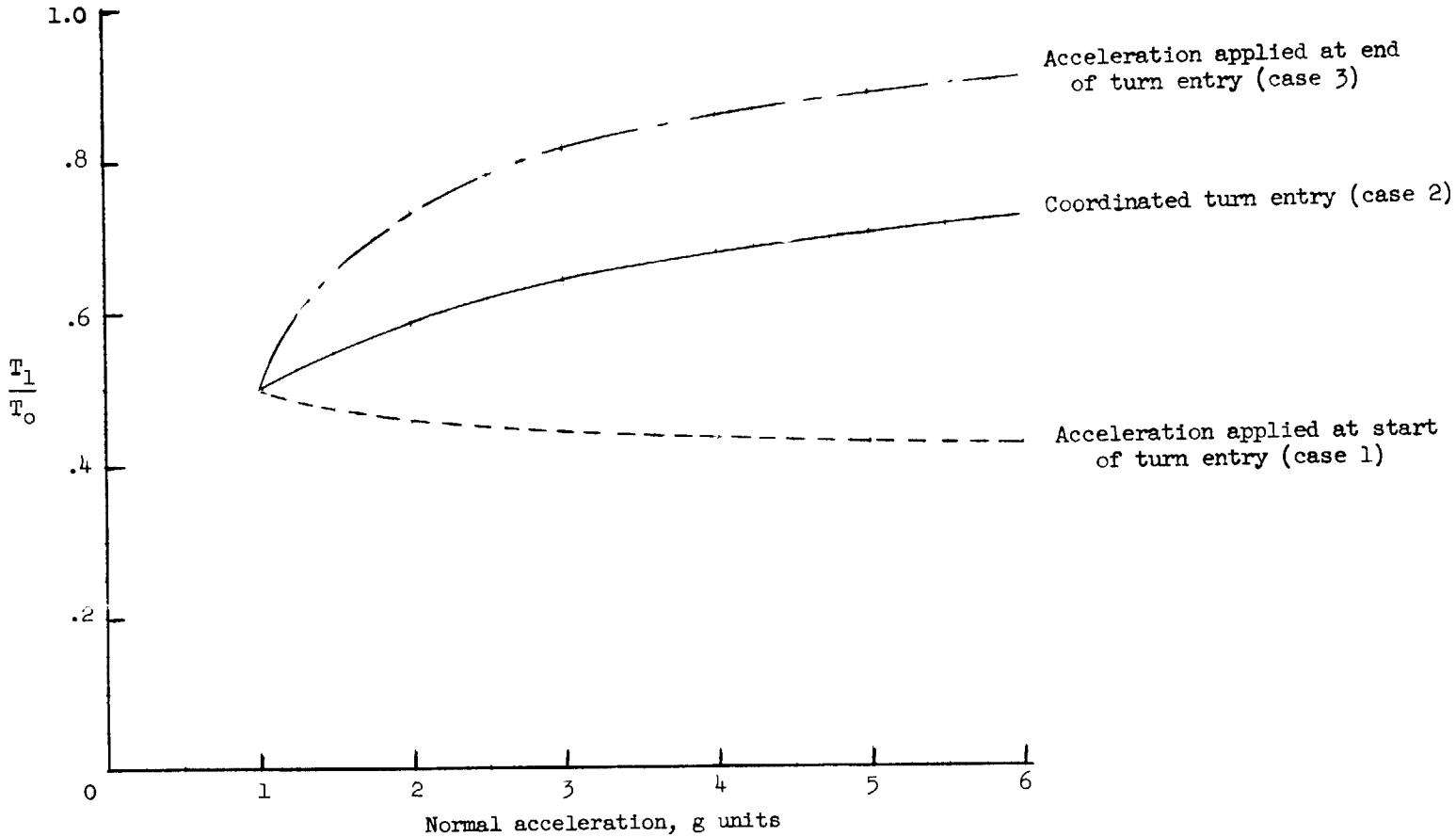

Figure 6.- Ratio of time of effective start of constant-radius turn to time required to reach steady bank angle T_1/T_o as a function of final normal acceleration for three types of variation of normal acceleration with bank angle.

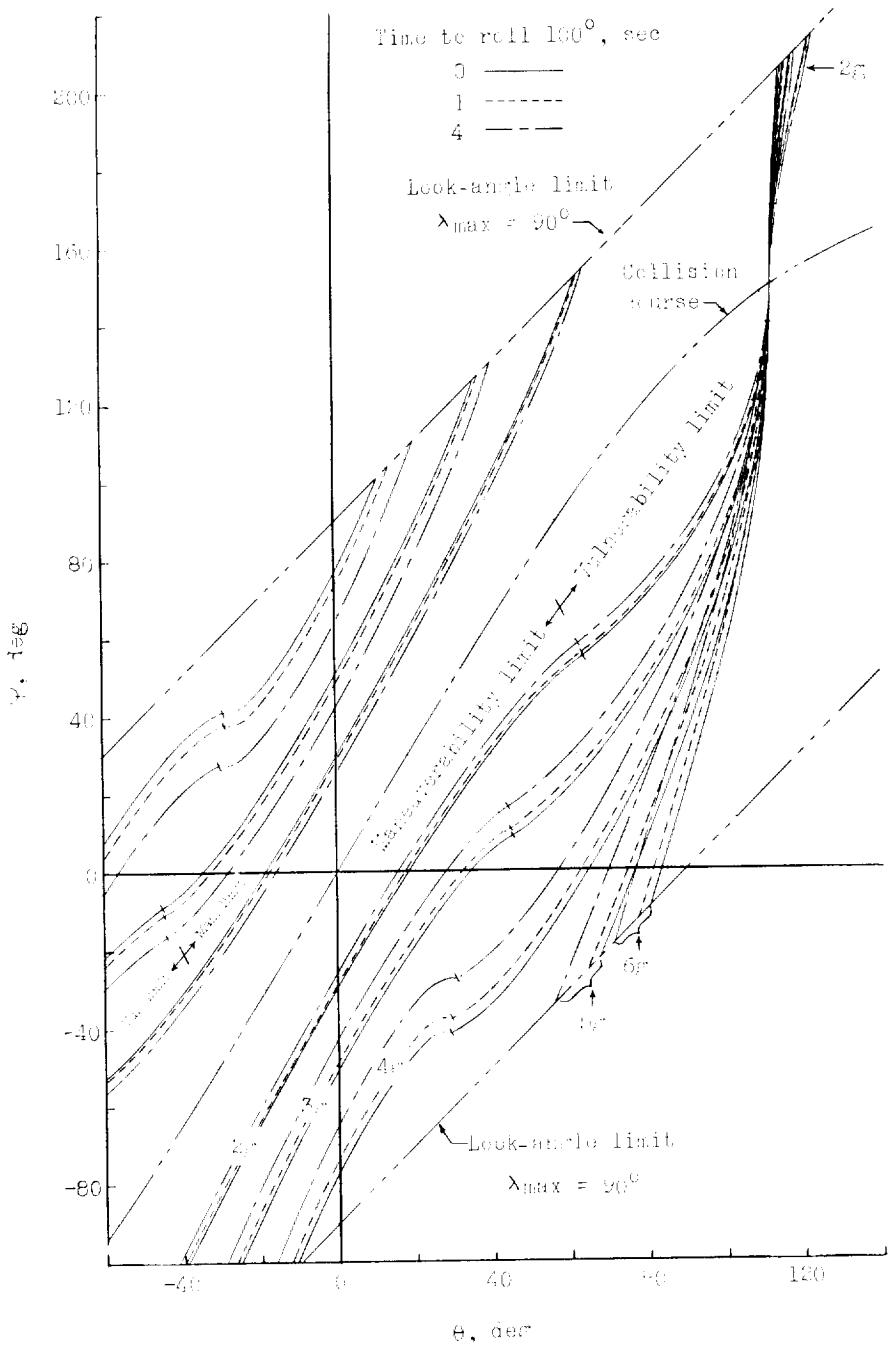

Figure 7.- Vectoring limits for a rocket-armed fighter flying at M = 1.5 attacking a target at M = 1.0. Relative effects of rolling performance and normal-acceleration capability are shown. Other conditions of encounter are given in table I.

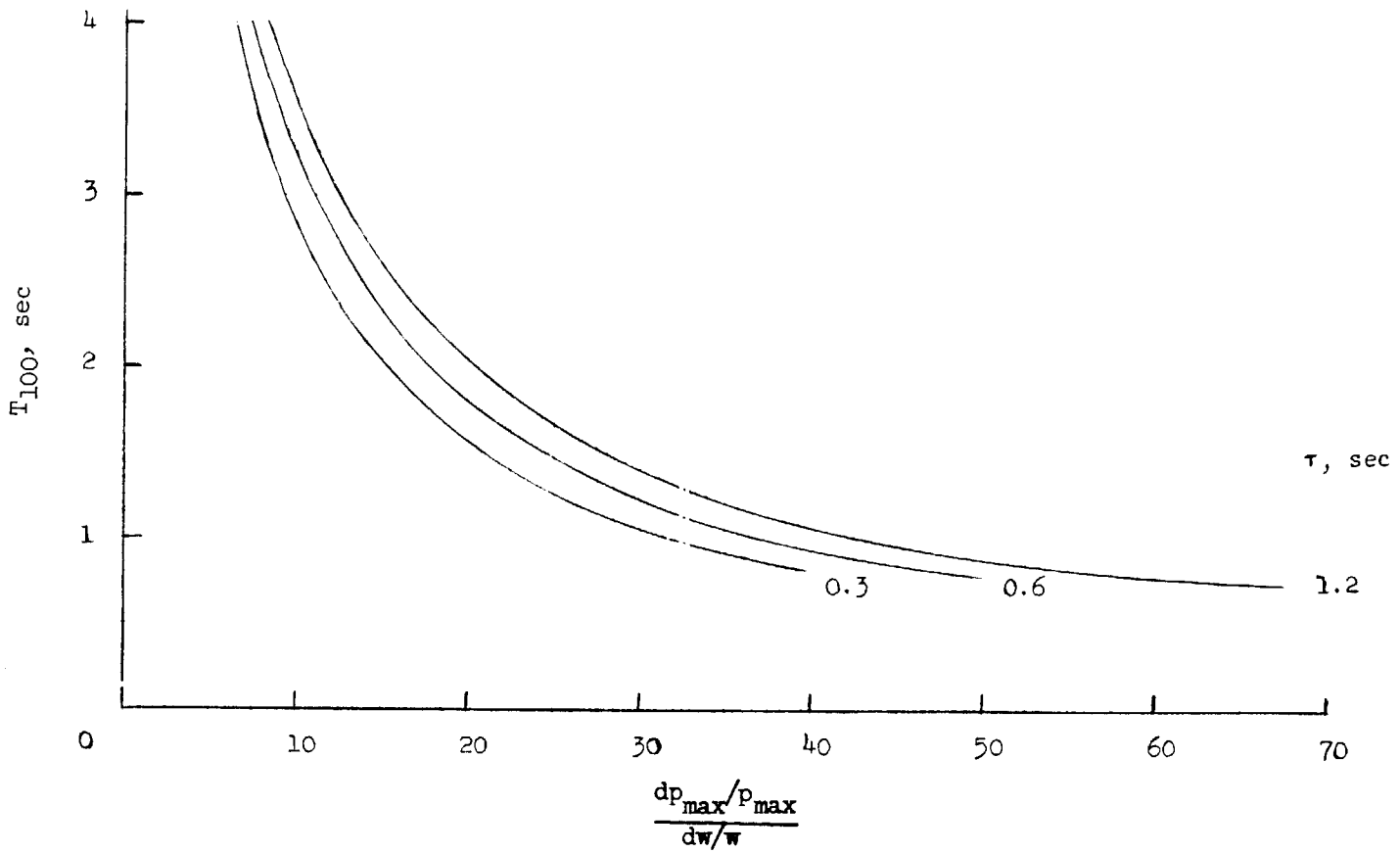

(a) No change in rolling inertia due to added weight $\left(\frac{d\tau/\tau}{dw/w} = 0\right)$.

Figure 8.- Variation of optimum time to roll through 100° as a function of $\frac{dp_{max}/p_{max}}{dw/w}$ for three values of τ.

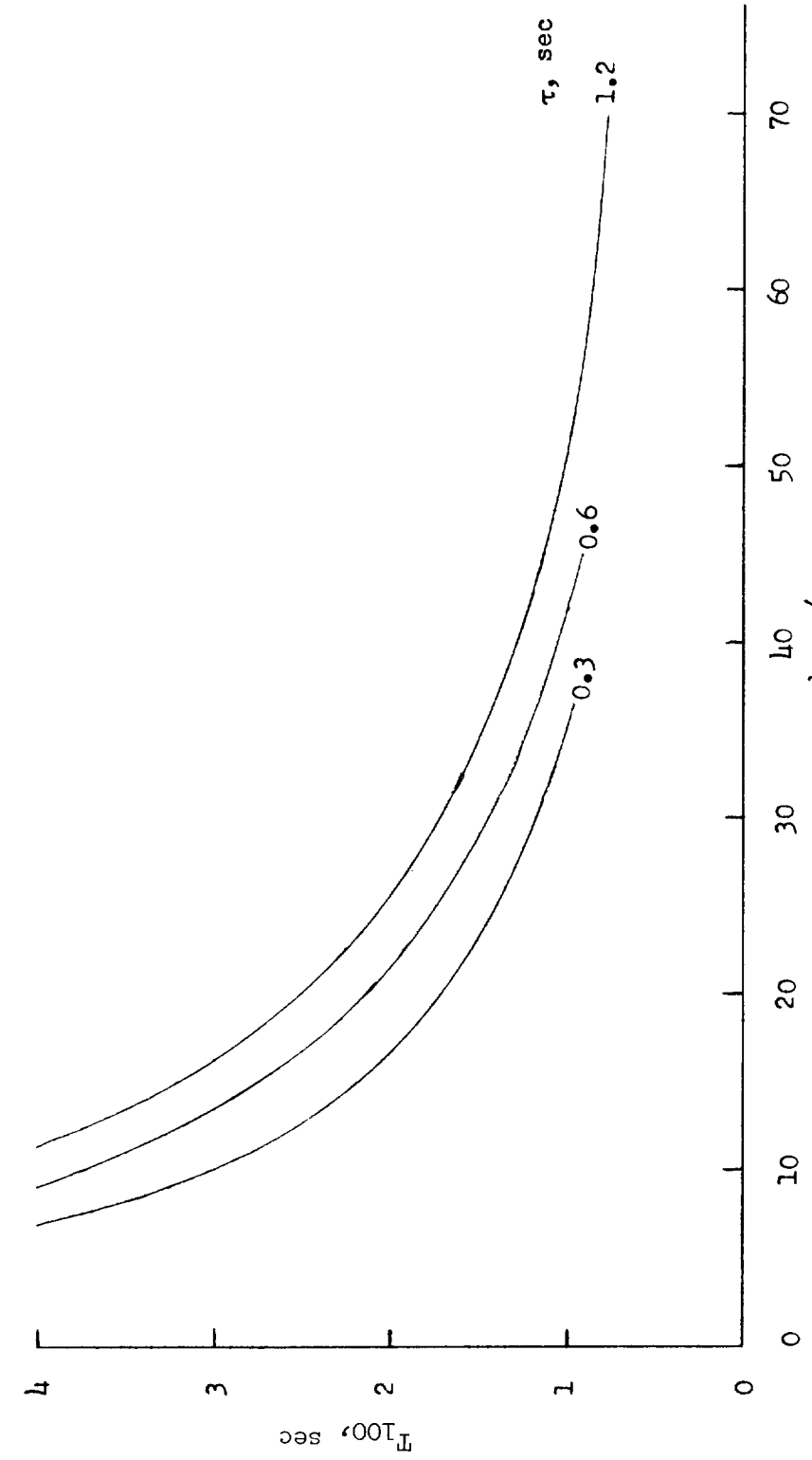

(b) Fractional increase in rolling inertia 10 times fractional increase in weight $\left(\frac{d\tau/\tau}{dw/w} = 10\right)$.

Figure 8.- Concluded.

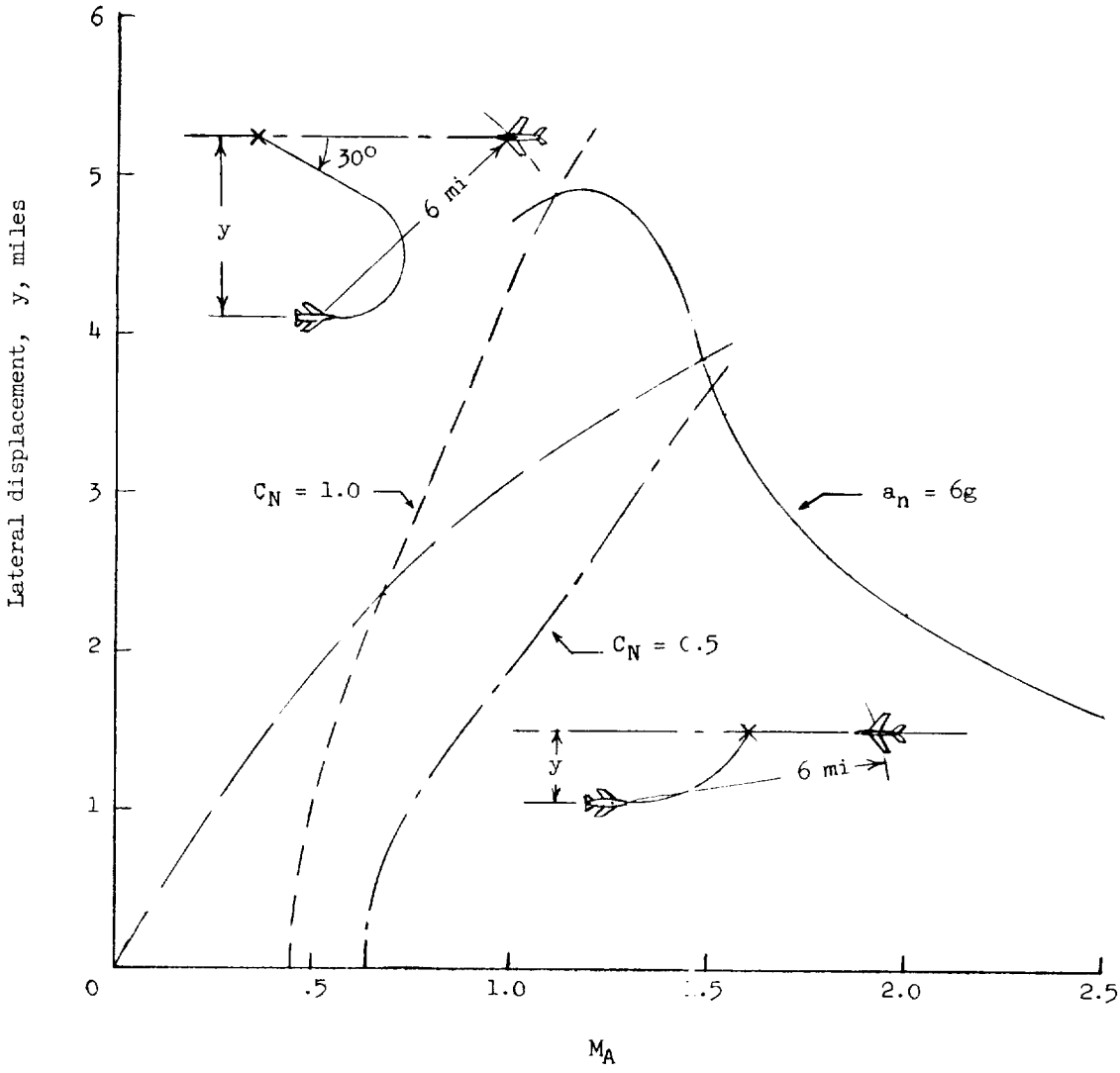

Figure 9.- Maximum lateral displacement from which an attack can be successfully completed as a function of attacker Mach number. Target Mach number = 1.0; radar range = 6 miles. Effects of limited normal-force coefficient and limited normal acceleration are shown. Long-dashed line divides plot into regions in which the attacker path includes or does not include a final straight segment with an angle of 30° to the target path.

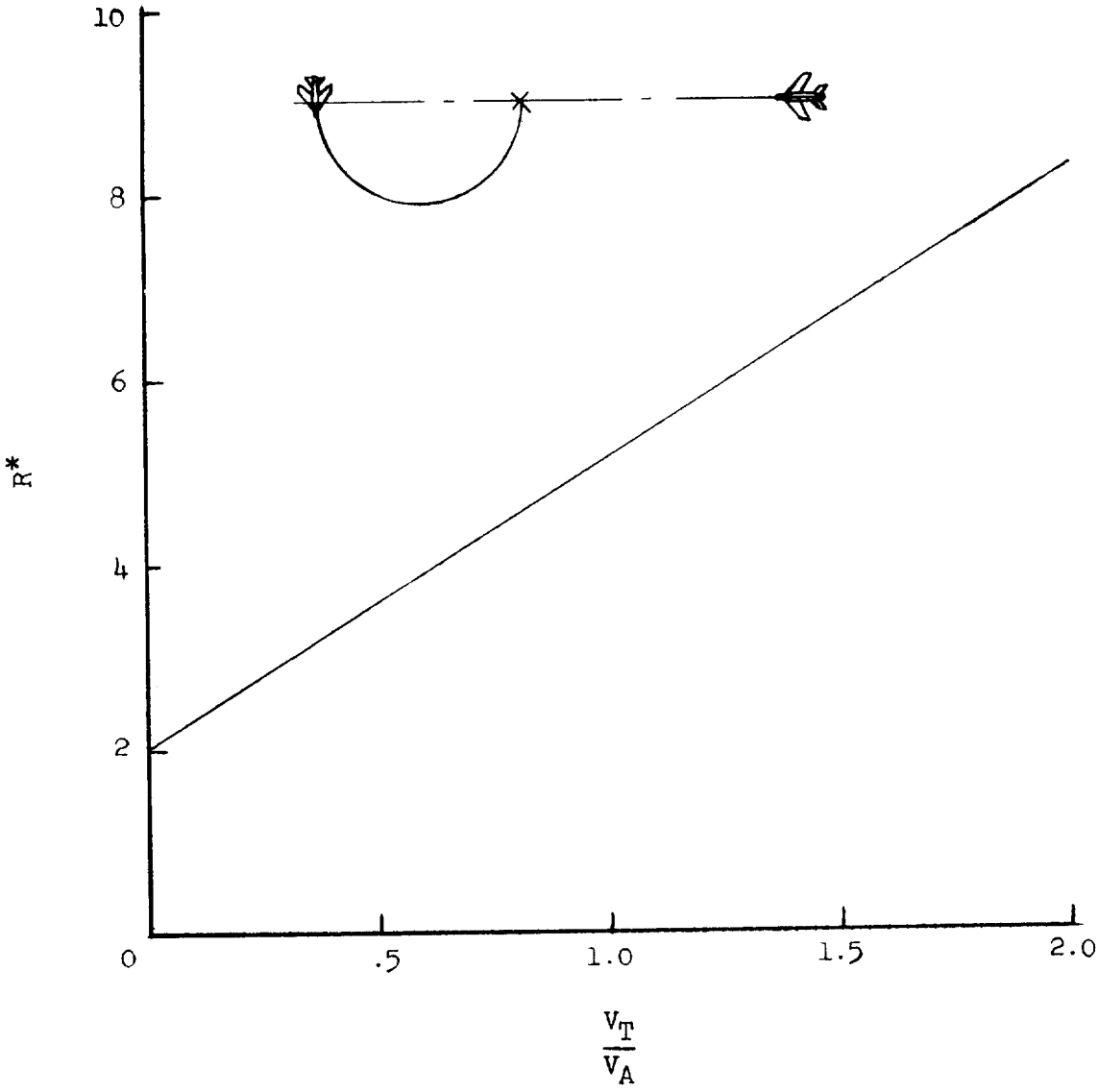

Figure 10.- Variation of ratio of radar range to radius of turn with ratio of target speed to attacker speed for the attack situation shown.

NASA - Langley Field, Va. L-1623